Atmos. Chem. Phys. Discuss., 11, 30419–30455, 2011
www.atmos-chem-phys-discuss.net/11/30419/2011/
doi:10.5194/acpd-11-30419-2011

Atmospheric Chemistry and Physics Discussions

The variability of urban aerosol size distributions and optical properties in São Paulo – Brazil: new particle formation events occur at the site

J. Backman[1], L. V. Rizzo[2], J. Hakala[1], T. Nieminen[1], H. E. Manninen[1], F. Morais[3], P. P. Aalto[1], E. Siivola[1], S. Carbone[4], R. Hillamo[4], P. Artaxo[3], T. Petäjä[1], and M. Kulmala[1]

[1]Division of Atmospheric Sciences, Department of Physics, University of Helsinki, Finland
[2]Department of Earth and Exact Sciences, Federal University of São Paulo, Brazil
[3]Institute of Physics, University of São Paulo, Brazil
[4]Finnish Meteorological Institute, Helsinki, Finland

Received: 29 September 2011 – Accepted: 26 October 2011 – Published: 11 November 2011

Correspondence to: J. Backman (john.backman@helsinki.fi)

Published by Copernicus Publications on behalf of the European Geosciences Union.

Abstract

The quest to reduce the dependence on fossil fuel has increased the use of bio-ethanol as an additive to gasoline. The metropolitan area of São Paulo (population 20 million) is a unique laboratory to study the ambient aerosol population caused by the use of bio-fuels because 55 % of the fuel used is ethanol. The use of ethanol as an additive to fossil fuel is known to increase aldehyde emissions and when photo chemically oxidized, result in smog. In order to characterize this smog problem total particle number concentration, particle number size distribution, light scattering and light absorption measurement equipment were deployed at the University of São Paulo campus area. Here we present the results from three months of measurements from 10 October 2010 to 10 January 2011. The median total particle number concentration for the sub-micron aerosol typically varies between 1×10^4–3×10^4 cm^{-3} frequently exceeding 5×10^4 cm^{-3} during the day. Median diurnal values for light absorption and light scattering vary between 12–33 Mm^{-1} and 21–64 Mm^{-1}, respectively. The hourly median single-scattering albedo varied between 0.63 and 0.85 indicating a net warming effect on a regional scale. A total of ten new particle formation (NPF) events were observed. During these events, growth rates ranged between 9–25 nm h^{-1}. On average, a calculated sulphuric acid vapour abundance of 2.6×10^8 cm^{-3} would have explained the growth with a vapour production rate of 2.8×10^6 cm^{-3} s^{-1} to sustain it. The estimated sulphuric acid concentration, calculated from global irradiance and sulphur dioxide measurements, accounted for only a fraction of the vapour concentration needed to explain the observed growth rates. This indicates that also other condensable vapours participate in the growth process. During the events, the condensation sink was calculated to be 12×10^{-3} s^{-1} on average.

1 Introduction

Atmospheric aerosols have been shown to affect human health and well-being (Nel, 2005). They influence visibility and the radiative forcing as they scatter (Cabada et al., 2004) and absorb (Jacobson, 2001) solar radiation. The effect can either be direct by scattering (Ramanathan et al., 2001) and absorbing (Ramanathan and Carmichael, 2008) solar irradiation or indirect by acting as a cloud condensation nuclei (CCN, Clarke and Kapustin, 2010; Lohmann and Feichter, 2005; Poeschl et al., 2010). The aerosol particles ability to affect these depends on their number concentration, size and chemical composition (Haywood and Boucher, 2000). They can either be emitted directly into the atmosphere or form there. New particle formation (NPF) depends on the abundance of gaseous vapours (especially sulphuric acid), the production of nanometer-size clusters and the pre-existing aerosol population (Kerminen et al., 2001; Kulmala, 2003). Condensable gaseous vapours can either grow existing particles or newly formed particles to sizes were they can act as CCN if they are abundant enough. In the initial formation, and growth, sulphuric acid is an important contributor (Sipilä et al., 2010). However, sulphuric acid concentrations can usually explain only a fraction of the observed growth rate (Kulmala et al., 2004).

Large urban conurbations are a significant source of aerosol particles and trace gases, with potential effects on the hydrological cycle (Lohmann and Feichter, 2005) and climate patterns (IPCC, 2007). Although they only cover a small area of land, they are a significant source of anthropogenic emissions. Atmospheric aerosols and trace gases are tightly connected via physical, chemical and meteorological processes. New ethanol based fuels for the worlds' vehicular fleet have been introduced to reduce the carbon dioxide footprint and our dependence on fossil fuels. However, there are uncertainties associated with their impact on air quality, human health and the climate (Farrell, 2006; Jacobson, 2007).

The metropolitan area of São Paulo (MASP, population 20 million) is a unique site for studying the impacts on air quality associated with the use of bio-fuels. The São

Paulo state environmental protection agency (CETESB, Companhia de Tecnologia de Saneamento Ambiental) has estimated that 55 % of the used vehicle fuel is in MASP is bio-ethanol. The MASP has a vast vehicular fleet counting 7.2 million which is powered by ethanol based bio-fuels. Previous studies have shown high concentrations of anthropogenic trace gases in São Paulo, many times higher than the polluted Los Angeles area in USA (Colon et al., 2001). CETESB has estimated that 97 % of the aldehyde emissions, 80 % of the hydrocarbon emissions and 40 % of the PM_{10} levels originate from the vehicular fleet in the area (CETESB, 2008). Photochemical interactions with volatile organic compounds (VOCs) and nitrogen oxides lead to ozone concentrations exceeding the World Health Organisation (WHO) limits of tolerance in São Paulo (Coêlho et al., 2010).

Ethanol as an additive to fossil fuel increase aldehyde emissions which result in a photochemical smog problem (Graham et al., 2008; Haagensmit, 1952; Seinfeld and Pandis, 2006). The smog is formed from precursor vapours which are oxidized in the atmosphere, resulting in species with low enough vapour pressures to be found in the condensed phase.

We know from previous studies that megacities differ from each other in terms of trace gas levels, particle emission, and ambient air quality (Gurjar et al., 2008; Laakso et al., 2006). The aim of the study is to characterize the number size distribution and total particle number concentration of the sub-micron aerosol population in the MASP. The observations reported are a part of the BIOFUSE ("The effects of intensive BIO-Fuel production and USE on regional air quality and global climate") project. The project is a collaborative effort between the University of Helsinki (UHEL), University of São Paulo (USP) and the Finnish Meteorological Institute (FMI). The results presented were measured between 10 October 2010 and 10 January 2011. We present diurnal patterns of the measured aerosol properties, and analyze the NPF events using trace gas and meteorological data. All times mentioned are in Universal Time Code (UTC) −3 h which is the local São Paulo wintertime and will be referred to as local time (LT).

2 Methods and instrumentation

2.1 The campaign measurement site

The site is located roughly 10 km from the city centre of São Paulo city, at the western edge of the most densely populated area. The urban city centre is surrounded by vast suburban residential areas populated by 20 million people. This makes São Paulo the worlds' 7th largest city. The city is located on a plateau 760 m above sea level (a.s.l.) surrounded by hills rising as high as 1200 m a.s.l. To the south east, about 60 km away, is the Atlantic Ocean. The climate is subtropical with dry winters (June–August) and wet summers (December–March). The measurements were made at the Armando Salles de Oliveira campus area of USP (Fig. 1). The campus area is vast, totalling an area of 7.4 km^2, making the site ideal for tracking ambient aerosols, without strong local sources. This should make the air masses arriving at the station well mixed and make the measurements representative of the ambient pollution burden of the city.

The measurement equipments were located on the roof of a four story building in a temperature controlled room. Air was sampled trough two equivalent sampling lines with $PM_{2.5}$ inlets mounted 0.5 m above the roof. Aerosol optical instruments were connected to one sampling line and total particle number concentration and particle number size distribution measurements were sampling through the other. Total particle number concentrations were measured with a condensation particle counter (CPC, Model 3022, TSI Inc, St. Paul, MN, USA, Sem et al., 2002) and number size distributions with a Differential Mobility Particle Sizer (DMPS, Hopke et al., 1978). A Neutral cluster and Air Ion Spectrometer (NAIS, Kulmala et al., 2007), also measuring size distributions, was placed outside in a cabinet with a sampling line of its own. The temperature of the cabinet was elevated above ambient to avoid condensation inside the instrument.

2.2 Supporting measurement stations

In addition to the measurements at the campaign site we took use of meteorological and trace gas measurements from existing measurements stations. The meteorological station closest to the campaign site was 100 m away at the Institute of Astronomy, Geophysics and Atmospheric Science (IAG, de Oliveira et al., 2002). The meteorological station is operated by the micrometeorology group at USP.

In addition, trace gas data provided by CETESB was used in the analysis. They maintain a network of atmospheric monitoring stations in the state of São Paulo. The closest available station measuring sulphur dioxide (SO_2) was the Osasco monitoring station located some 6 km away, in a suburban surrounding. The other two monitoring stations (Congonhas and Cerqueira Cesar), also fairly close to the campaign site, but based on our assessment, were discarded for being in too different surroundings in comparison to the campaign site.

2.3 Instrumentation

2.3.1 Differential Mobility Particle Sizer (DMPS)

Sub-micron aerosol number size distribution and total number concentration was monitored with a DMPS system (Aalto et al., 2001). To minimize diffusion losses two aerosol flow arrangements were used in the same Vienna-type Differential Mobility Analyzer (DMA, Winklmayr et al., 1991) with closed sheath flow arrangements. The DMPS was set to measure number size distributions from 6–800 nm mobility diameters. For the smaller particles a high aerosol flow of 4 l min^{-1} and a sheath flow of 20 l min^{-1} were used to measure mobility diameters from 6–280 nm. Mobility diameters from 100–800 nm were measured with an aerosol flow of 1 l min^{-1} and a sheath flow of 5 l min^{-1}. These flow rates result in the same non-diffusional transfer function with a β of 1/5 as described by Zhang and Flagan (1996).

The high voltage supply for the DMA was calibrated between 0 and 1 kV and a similar slope was assumed for the whole range. This was verified by sampling 404 nm latex particles and changing the sheath flow of the DMA. The calibration of the CPC used in the DMPS system is described in the calibration section of this paper.

2.3.2 Neutral cluster and Air Ion Spectrometer

To be able to track the initial steps of NPF and the processes associated with these a Neutral cluster and Air Ion Spectrometer (NAIS) was deployed. NAIS measures mobility distributions in the range 3.2–0.0013 $cm^2\,V^{-1}\,s^{-1}$ which corresponds to mobility diameters ranging from 0.8–42 nm (Mirme et al., 2007). The instrument is a further development of the Air ion Spectrometer (AIS) which only measures naturally charged particles. The ability of NAIS to measure neutral clusters arises from the unipolar corona chargers. In the neutral particle mode, the particles are charged with corona chargers and the charging probability is calculated using Fuchs theory (Fuchs, 1963). Before the sample enters the DMA's some of the corona charger ions are filtered out using electrical post-filters. Mobility distributions are measured with two DMA's in parallel, one for each polarity. The central electrodes of the DMA's have a polarity opposite to the charger surrounded by 21 circular electrometers. The oppositely charged particles entering the vicinity of the DMA precipitate onto the outer walls away from the central electrode onto the electrometers. Electrometer currents are inverted to 28 different size bins taking into account experimentally determined diffusion losses and instrument noise. The noise of the electrometers are measured subsequently and then subtracted from the measurements thus minimizing the influence of any reduction in electrometer performance. A schematic of the instrument is presented in Manninen et al. (2009b).

The post-filters are manually tuned so that not all of the main charger ions are removed so that the instrument performance can be tracked better. Combined DMPS and NAIS number size distributions were plotted from 3–800 nm, thus discarding these charger ions. Although the NAIS and DMPS measure the same aerosol the inversion,

charging probability, and charging method differ.

2.3.3 Optical properties

The optical properties tracked were light scattering coefficients and black carbon (BC) mass concentrations. These were measured with a nephelometer (Model 3563, TSI Inc., St. Paul, MN, USA) and a Multi Angle Absorption Photometer (MAAP, Model 5012, Thermo Scientific, Franklin, MA, USA). The aerosol was dried with a diffusion drier.

The nephelometer measures light scattering coefficients at 450, 550, 700 nm wavelengths (Anderson and Ogren, 1998). Scattering coefficients were corrected for angular truncation error according to Anderson and Ogren (1998). Instrument calibration was done using particle free air and carbon dioxide. Scattering coefficients measured with a relative humidity (RH) exceeding 50 % were discarded, which was less than 30 % of the dataset.

BC concentrations measured with the MAAP were measured at a wavelength of 637 nm (Petzold et al., 2005). The BC mass concentrations of the MAAP were calculated to light absorption coefficients using mass absorption cross-section (MAC) system value of 6.6 $m^2\,g^{-1}$. Furthermore, as suggested by Müller et al. (2011), a 5 % increase in light absorption was applied.

Both instruments were calculated to 1000 mbar and 0 °C conditions from the nephelometer data. Using Ångström exponents, light scattering was interpolated to the MAAP wavelength yielding the single-scattering albedo of the aerosol.

2.3.4 Instrument calibrations

Prior to deployment, the CPC's were calibrated with the aid of an electrometer (Model 3068, TSI Inc., St. Paul, MN, USA). The calibration setup was principally the same as is described in the technical paper by Agarwal and Sem (1978). Silver particles were produced by heating silver in an oven to 1000–1060 °C in a nitrogen atmosphere.

The calibration setup was used to determine the particle number concentrations and

cut-off diameter of the CPC's against the reference electrometer in the single particle counting mode (10^3–10^4 cm^{-3}). Ideally, the particle number concentrations measured with the CPC's and the electrometer would be the same (slope 1 : 1). The slope was determined with 50 nm particles, well above the cut-off diameter of the CPC's. In photometric mode, the CPC's were compared against each other onsite with 50 nm sodium chloride particles and operated side-by-side with the DMPS.

The cut-off diameters were determined both with and without aerosol driers inline. In this way we were able to estimate the effect of diffusional losses in the driers, represented by an equivalent length of tube losses in the sampling line. The CPC (Model 3772, TSI Inc., St. Paul, MN, USA) used in the DMPS had a cut-off diameter of 6 nm. With the NAPHION (Permapure LLC, Toms River, NJ, USA) diffusion drier in the DMPS the cut-off size was 13 nm. From these results the equivalent length of the drier was calculated to be 13.3 m. The cut-off diameter of the TSI 3022 CPC was 5 nm. With its Topas (Topas GmbH, Dresden, Germany) diffusion drier the cut-off was at 7 nm. This was calculated to be equivalent to 2.7 m of sampling line.

2.4 New particle formation event analysis

New particle formation (NPF) depends on the competition between the initial growth of the nuclei and their scavenging by the pre-existing particulate population (Kulmala et al., 2005). The condensation sink (CS) is a measure of the molecule loss from gas phase to the existing particle surface via condensation (Dal Maso et al., 2002; Kulmala et al., 2005). When the CS is low, also small condensable vapour source rates (Q) are enough for small particles to form and grow. However, when the CS is large, the vapour abundance needed for the particles to form, grow, and survive to observable sizes need to be substantially larger (Kulmala et al., 2005). While CS can be a limiting factor for NPF, the fact that these events occur at heavily polluted areas proves a large abundance of condensable vapours. In this study, the vapour concentration (C_{vap}) needed to explain the growth was calculated using Eq. (8) in Nieminen et al. (2010) for sulphuric acid (H_2SO_4). To sustain the observed growth, the production rate (Q) of the

condensing vapours was calculated as $Q = \mathrm{CS} \cdot C_{\mathrm{vap}}$.

The NPF event days and the formation rates of particles were determined according to the method described by Dal Maso et al. (2005). The formation rate (J) was calculated using particle concentrations in the size range 6–20 nm for the DMPS data and 2–3 nm for the NAIS data, denoted J_6 and $J_{2,\mathrm{TOT}}$, respectively. The formation rate of 6 nm particles (J_6) can be expressed as

$$J_6 = dN_6/dt + \mathrm{CoagS} \cdot N_6 + \mathrm{GR}/\Delta d_{\mathrm{p}} \cdot N_6 \cdot \quad (1)$$

Here N_6 is the number concentration of 6–20 nm particles, CoagS is the coagulation sink of the pre-existing particles, Δd_{p} is the width of the 6–20 nm size range, and the growth rate (GR) of the particles in the same size range. CS is calculated from the particle number size distributions with the method presented by Kulmala et al. (2001). For the growth rate calculations we first determined the times of the concentration maxima in each of the size bins. Linear least-square fits were made to these points. The slope of these fits is the GR. A more thorough description of the method is given by Hirsikko et al. (2005).

The NAIS also measures naturally charged particles down to 0.8 nm in diameter, thus enabling us to observe the first steps of NPF events. The calculations of 2 nm ion formation rates (J_2) from 2–3 nm ion concentrations (of both polarities) were done according to Manninen et al. (2009a) as

$$J_2^{\pm} = dN_2^{\pm}/dt + \mathrm{CoagS} \cdot N_2^{\pm} + \mathrm{GR}/\Delta d_{\mathrm{p}} \cdot N_2^{\pm} + \alpha \cdot N_2^{\pm} \cdot N_2^{\mp} - \beta \cdot N_2 \cdot N_2^{\pm} \quad (2)$$

were the superscripts ± denote the particle charge. There are now two additional terms in comparison to Eq. (1). Additional losses for the ions occur via ion-ion collisions, which was estimated assuming a recombination coefficient (α) value of 1.6×10^{-6} cm^3 s^{-1} (Tammet and Kulmala, 2005). Ion-neutral attachment was taken into account with the ion-neutral attachment coefficient (β) of 10^{-8} cm^3 s^{-1} (Tammet and Kulmala, 2005).

Sulphuric acid is very likely closely linked to atmospheric NPF (e.g., Weber et al., 1996). As no measurements of sulphuric acid were measured at the campaign site,

we estimated the concentrations using the method presented by Petäjä et al. (2009). In steady-state conditions the proxy for sulphuric acid concentration is

$$H_2SO_4 = k \cdot [SO_2] \cdot \text{GlobRad}/\text{CS}. \quad (3)$$

Here $[SO_2]$ is the sulphur dioxide concentration, GlobRad is solar radiation intensity, and CS the condensation sink by the pre-existing aerosol. For the scaling factor k we used a value of $1.4 \times 10^{-7} \cdot \text{GlobRad}^{-0.7}\,\text{m}^2\,\text{W}^{-1}\,\text{s}^{-1}$. This is based on measurements in a boreal forest environment in Finland (Petäjä et al., 2009), and therefore should be considered as relative abundances rather than precise absolute concentrations.

3 Results and discussion

The results presented were measured during 10 October 2010 and 10 January 2011 and are representative of the spring and early summer in São Paulo region. In spring, bursts of intense rainfall become gradually more frequent, and reach a maximum in February.

3.1 Total particle number concentration

The three month average total particle number concentration was $20.1 \times 10^3\,\text{cm}^{-3}$ (standard deviation $11.0 \times 10^3\,\text{cm}^{-3}$). This is roughly half of what has been measured in springtime in Beijing in 2004 ($54 \times 10^3\,\text{cm}^{-3}$, Wehner et al., 2004). In comparison, Hyvärinen et al. (2010) reported a mean concentration of $22.6 \times 10^3\,\text{cm}^{-3}$ for a rural site 25 km from the centre of New Delhi. The maximum 24 h average concentration during autumn in New Delhi (Mönkkönen et al., 2005) was twice as high ($6.28 \times 10^4\,\text{cm}^{-3}$, standard deviation $1.78 \times 10^4\,\text{cm}^{-3}$) in comparison to $3.37 \times 10^4\,\text{cm}^{-3}$ (standard deviation $3.37 \times 10^4\,\text{cm}^{-3}$) which we measured in São Paulo.

There is a clear diurnal pattern in the total particle number concentration (Fig. 2a) and the nucleation, Aitken, and accumulation mode particles (Fig. 2b). This is what we

would expect since the largest single source of sub-micron particles is traffic related. Figure 2a shows that the median night time total particle concentration is between 1.2×10^4–$1.7 \times 10^4\,\text{cm}^{-3}$ from midnight to 06:00 LT. During office hours (07:00–15:00 LT), the median concentrations reach up to $2.9 \times 10^4\,\text{cm}^{-3}$. In the evening the median values were typically $1.6 \times 10^4\,\text{cm}^{-3}$. Worth noticing are the variations in the statistical edges indicated with black whiskers in the figure. No precipitation data were available so we can only make educated guesses on the origin of these extremes. Increased wet deposition due to intense precipitation partly explains the lower extremes, while the upper extremes are likely to originate from NPF events or anthropogenic emissions (Allen et al., 2009; Hyvärinen et al., 2009; Hyvärinen et al., 2010).

Figure 2b represents the diurnal evolution of number concentration of nucleation mode (6–25 nm), Aitken (25–90 nm) and accumulation modes (90–800 nm). The nucleation mode particles explain a large fraction of the variation in the total particle number concentrations. In the evening the total number concentration is dominated by Aitken mode particles. The accumulation mode particles peak in the afternoon and they account for only a small fraction of the total particle number concentration.

Particle concentration as a function of week day is presented in Fig. 3. In general, the weekend particle number concentrations were lower than during weekdays, because there is less traffic during weekends (Silva Júnior et al., 2009). Sunday had the lowest and Friday the highest median particle number concentrations, 1.3×10^4 and $2.3 \times 10^4\,\text{cm}^{-3}$, respectively.

3.2 Particle number size distributions

The median particle number size distribution during the measurement period is shown in Fig. 4. A peak of the median number size distribution is at 24 nm. We fitted three modes to the size distribution with the method described by Hussein et al. (2005). Based on the median number size distribution, the nucleation mode is responsible for most of the particles by numbers. The modal peak of the nucleation mode was at 18 nm. The Aitken mode particles in the size distribution had a peak at 50 nm and the

accumulation mode peaked at 206 nm. The median particle number concentrations for the nucleation, Aitken and accumulation modes were 8600, 6900, and 500 cm^{-3}, respectively. The widths (σ) of the modes were calculated to be 1.96 for nucleation mode, 1.99 for Aitken mode and 1.40 for the accumulation mode particles.

Furthermore, count mean diameters (CMD) and surface mean diameters (SMD) were calculated from size distribution measurements. These reflect the diurnal behaviour associated of the aerosol dynamics, pollution sources, and boundary layer conditions. Firstly, traffic is the most intense during office hours (Fig. 2), and there is a morning and an afternoon rush hour. Traffic is the dominant source of primary aerosol particles. Secondly, atmospheric stability plays a vital part in ground level pollution (both trace gas levels and particle concentrations). At dusk, a nocturnal layer can be formed, and breaks up after dawn, when solar irradiance induces convective mixing. A stable nocturnal boundary layer suppresses the mixing of ground level pollution with the residual layer above. Depending on how strong the thermal convection is, the mixing height can vary. The higher the mixing height, the more the ground level concentrations gets diluted with the residual layer above. Evidently, this happens during morning rush hours (Fig. 5). At night, when there is less emission of primary particles, and little convection, physical processes grow the pre-existing particles. They grow in size by coagulation and condensation. This can be seen from Fig. 5, were both CMD and SMD have their maximum at night. During the day, freshly emitted primary particles dominate. Then, particles that grew during the night have been mixed trough out the mixing layer, explaining the low CMD and SMD values during the day. The same behaviour has been reported for New Delhi. There the geometric mean diameter (GMD) was low in the afternoon and increased into the night (Mönkkönen et al., 2005).

3.3 Aerosol optical properties

Aerosol optical properties are of climatological significance (Haywood and Boucher, 2000). In Fig. 5, the diurnal patterns of light scattering coefficients (σ_{SP}), light absorption coefficients (σ_{AP}), single-scattering albedo (ω_0), and light scattering Ångström

exponents (α_{SP}) are plotted. The optical properties σ_{SP}, σ_{AP}, and ω_0 are reported at a wavelength of 637 nm. Ångström exponents were calculated from σ_{SP} measured at 450 and 700 nm wavelengths. Furthermore, the diurnal behaviour of CMD and SMD were plotted in the same picture to show how they relate to the optical properties of the aerosol. All of these show a clear diurnal pattern.

During the course of the day, hourly median values for σ_{SP} and σ_{AP} vary between 21–64 Mm^{-1} and 12–33 Mm^{-1}, respectively. This is in the same range (σ_{SP} = 53 Mm^{-1} and σ_{AP} = 21 Mm^{-1} mean values at 525 nm) as a remote site in northern India, mostly dominated by long range transport, i.e. the brown cloud in Asia (Hyvärinen et al., 2009). In São Paulo, both coefficients show a peak in the morning (07:00 LT) and coincide with the morning rush hour. A similar behaviour has been reported for Beijing (Garland et al., 2009) and for carbonaceous aerosol in Mexico City (Salcedo et al., 2006). The fact that light scattering and absorption coefficients both peak indicates the predominance of primary aerosols (Paredes-Miranda et al., 2009). Both coefficients have minimums in the afternoon. The same behaviour has been reported for Beijing (Garland et al., 2009) and continental Europe (Mészáros et al., 1998).

The single scattering albedo (ω_0) calculated from σ_{SP} and σ_{AP} (at 637 nm) show a decrease in the morning (minimum at 07:00 LT) and then a peak in the afternoon (13:00 LT). The minimum in the morning was 0.63. The minimum is consistent with the absorption peak discussed earlier, indicating a significant contribution of soot particles to the aerosol population. During morning rush hour it is likely that the night time boundary layer has not yet fully broken up while traffic is already heavy. When it breaks up, the pollution is diluted due to convectional mixing, and absorption coefficients decrease at ground level. This hypothesis is supported by the fact that both CMD and SMD are at their minima in the afternoon. When the total particle number concentrations are the highest (Fig. 2) both CMD and SMD have their minimums (Fig. 5e–f). It implies that the primary soot aerosols from the vehicular fleet are small in size and dominant in number.

After the morning rush hour, when convectional mixing increases and photochemistry come into play, ω_0 experiences a gradual increase reaching a peak median value of 0.85 at 13:00 LT. In the evening, there is a gradual decrease again, probably due to evening rush hour. According to Ramanathan et al. (2001), ω_0 values below 0.85 result in a positive climate forcing with a warming effect due to absorbing aerosols. Furthermore, if they are abundant enough, they may affect the vertical temperature structure in the troposphere with implications to atmospheric convection and cloud formation (Hansen et al., 1997; Herrmann and Hänel, 1997). The low ω_0 values presented here indicate that the City of São Paulo has a direct net warming effect on a regional scale.

Median values of the scattering Ångström exponents (α_{SP}) range between 1.3 and 1.67 during the day (Fig. 5d). α_{SP} is dependent on particle size and therefore the number size distribution of the aerosol. Values greater than 1.0 are typically associated with fine mode particles from incomplete combustion processes. Values lower than 1.0 are typically associated with large particles like sea salt and dust (Eck et al., 1999). When compared, SMD and the size dependent α_{SP} reflect the same behaviour of the aerosol. When the SMD is low, α_{SP} is high and vice versa.

3.4 New particle formation events

NPF events have been observed all over the world, from pristine atmospheric conditions in Antarctica (Virkkula et al., 2007) to heavily polluted continental areas like Mexico City, Mexico (Kalafut-Pettibone et al., 2011), New Delhi, India (Hyvärinen et al., 2010), in the Himalayas (Neitola et al., 2011), and oceanic NPF events in the South Pacific (Kulmala et al., 2004, and references therein). We show that NPF events also occur in such heavily polluted areas as São Paulo. Out of ten NPF events (Table 1), four class Ia events could be further analyzed. The class Ib events observed had initial sizes between 10 and 20 nm and were not used in the analysis. These events were likely local NFP events passing by the measurement station which would explain the absence of the initiation of the event. One class II type event was observed on 12 October 2010.

A summary of the parameters derived from the NPF events as described in the methods section of this paper is given in Table 1. We chose to compare our results with results from New Delhi, India (Mönkkönen et al., 2005), Beijing, China (Wehner et al., 2004), and Mexico City Mexico (Dunn et al., 2004; Kalafut-Pettibone et al., 2011). In São Paulo, we observed GR between 9 and 25 nm h^{-1}. In New Delhi, India similar GR have been observed (11–18 nm h^{-1}, Mönkkönen et al., 2005). Also similar GR have been reported for Mexico City (Kalafut-Pettibone et al., 2011) ranging from 6–18 nm h^{-1}. This is an order of magnitude higher GR than what has been reported for a remote site in the Indian Himalayas (Neitola et al., 2011). Mönkkönen et al. (2005) reported NPF with a CS of $50–70 \times 10^{-3}$ s^{-1} which is by a factor of 3–11 more than what was measured in São Paulo, $6–17 \times 10^{-3}$ s^{-1}. Similarly, the vapour production rate in New Delhi (9×10^6–14×10^6 cm^{-3} s^{-1}) was up to one order of magnitude more than for São Paulo ($1.5–3.5 \times 10^6$ cm^{-3} s^{-1}). In contrast to NPF in pristine conditions (e.g., Dal Maso et al., 2005), we observed NPF events with a much higher pre-existing aerosol population of 2×10^4 cm^{-3} on 2 November 2010 (Fig. 6).

The most intense (Class Ia) NPF event observed had a GR of 9.3 nm h^{-1}. The particle number size distributions measured during the event are presented in Figs. 6 and 7. The event begins at 09:00 LT. Due to the fast growth of the particles the events show up roughly the same time in both instruments. In Fig. 6 we can see a similar drop in total aerosol surface area before the event begins as was seen in Beijing, China (Wehner et al., 2004). The sulphuric acid proxy concentration (H_2SO_4) shown in the lower panel of Fig. 7. H_2SO_4 proxy starts to increase already at 08:00 LT, an hour earlier than the NPF event. Later, when the H_2SO_4 proxy concentration decreased just before noon, no new particles are formed, while the freshly nucleated particles continue to grow into larger sizes. There are two possibilities for this behaviour. Either there is a threshold H_2SO_4 concentration of approximately 5×10^6 cm^{-3} or the trace gas monitoring station further away measures another air mass (time delay). Furthermore, when there are no more nucleating vapours, the solar irradiation still increases to a maximum between 11:00 and 12:00 LT. The decline in the sulphuric acid proxy between 09:00 and 10:00 LT

is due to less SO_2, not solar irradiation. Increasing mixing height due to thermal convection, as the day grows older, mixes ground level SO_2 troughout the boundary layer (Fig. 8). This reduces H_2SO_4 concentrations which are closely linked to NPF.

Since the trace gas monitoring station (used to derive H_2SO_4 the proxy) is some 6 km away from the measurement site it adds uncertainties to both the timeframe and absolute concentrations. However, from a rose plot (not included), the origin of the SO_2 is the city centre. As both the H_2SO_4 proxy and the NPF event match, we can expect to have nucleating particles at both stations. At a boreal forest environment in Finland, Nieminen et al. (2009) reported an order of magnitude lower threshold concentration of 3×10^5 cm^{-3} based on measured H_2SO_4. The H_2SO_4 concentration needed to explain the growth in São Paolo, was on average, 2.6×10^8 cm^{-3} (Table 1). The average H_2SO_4 proxy concentration was over an order of magnitude less (1.1×10^7 cm^{-3}). However, still considering the uncertainties, there are most likely other vapours (e.g. organics) present in these NPF events contributing to particle growth (Jimenez et al., 2009; Orlando et al., 2010). This is consistent with observations at other locations (Kulmala et al., 2001; Wehner et al., 2005).

3.5 Evaporation from sub-micron particulate matter

The growth of particles by condensable vapours is dependent on their abundance. To find these vapours in the condensed phase, their mixing ratio must exceed their saturation level. Oxidation lowers the saturation vapour pressure of the gases, thus making them more likely to condense. If the condensational growth of particles stops, the gas to particle (and vice versa) interactions are at steady state. Should the atmospheric conditions change in a way that the concentration of the precursor vapour decreases, the condensed species start to evaporate, making the particles shrink in size.

We observed that the ambient sub-micron particle modes decreased in size between 14:00 and 17:00 LT on the 12 October 2010 (Fig. 9). These shrinking modes could be due to evaporation of semi-volatile species from the particulate phase as atmospheric

conditions change. We can see that the existing population of 36 nm particles shrink, most probably by evaporation, to 16 nm (Fig. 9). The rate of shrinking was calculated to be 5.2 nm h^{-1}. Shrinking accumulation mode particles can also be seen, however not as clearly, starting before noon. The global irradiance data suggest that during morning hours, until 11:00 LT, it was partly cloudy (Fig. 9). After 12:00 LT, when there was little or no cloud cover. Either the stable nocturnal boundary layer broke up or the boundary layer mixing height increased. Thus, diluting total particle concentrations and the trace gases, explaining the observed evaporation. No atmospheric stability parameters were available but both of these plausible cases result in the same dilution of near ground level concentrations.

In this case, atmospheric conditions seem to change more rapidly than the vapour pressure decreases by photochemical oxidation. No mass spectra of these particles were measured, so it remains unclear which vapours were evaporating.

4 Conclusions

The use of bio-ethanol as an alternative fuel is envisioned to lessen our dependence on fossil fuels in urban transportation. However, there are uncertainties associated with their use, and they need to be addressed. The huge area of São Paulo has a population base of 20 million, and a large vehicular fleet (7.2 million). These vehicles use bio-ethanol as an additive which results in increased precursor vapours that form smog via photochemical processes. We tracked particle number size distributions, total particle number concentrations and optical properties to get a better understanding of the air pollution of the city. Our data can further be used to assess the impact on the local climate and human health (Davidson et al., 2005; Lohmann and Feichter, 2005; Ramanathan and Carmichael, 2008).

Our measurements show clear diurnal patterns in sub-micron aerosol number size distribution and aerosol optical properties in São Paolo, Brazil. Hourly median total particle number concentrations were close to 3×10^4 cm^{-3} during the day, and frequently

exceeding 5×10^4 cm^{-3}. The particle number size distribution data suggest that nucleation, and Aitken mode particles dominate the particles by number. The nucleation mode particles show a diurnal pattern similar to the total particle number concentration. Aitken mode particles do not. The Aitken mode particles are likely to originate from coagulated and coated nucleation mode particles and primary anthropogenic emission. Light scattering and light absorption coefficients also show diurnal patterns. They both peak during morning rush hours when the single-scattering albedo is low. Hourly median light scattering and absorption coefficients range between 21–64 Mm^{-1} and 12–33 Mm^{-1}, respectively. The hourly median single-scattering albedo, significant to the aerosol radiative forcing, ranged between 0.63 and 0.85. This suggests a direct net warming effect by the pollutants on a regional scale. Both the light scattering, light absorption and particle number size distribution measurements illustrate the daily evolution of the particles as they are emitted, grow by condensation and coagulation, and are diluted by convection in the boundary layer. The observed cycle is related to boundary layer meteorology, photochemistry, and the physical processes governing the fate of these particles but their unique roles in São Paulo remains to be quantified.

During the three month period we found ten new particle formation events, which were classified. Four of these could be further analyzed in order to explain the conditions associated with the events in the city. GR in São Paulo were similar to those reported for Mexico City (Kalafut-Pettibone et al., 2011) and New Delhi (Kulmala et al., 2005; Mönkkönen et al., 2005). We found a large CS during NPF events in comparison to pristine conditions. However, the CS during NPF events in New Delhi was by a factor of 3–11 times higher than in São Paulo. Consequently the vapour production rate replenishing the condensable vapours was an order of magnitude lower in São Paulo in comparison to New Delhi. The vapour abundance was estimated to be 2.6×10^8 cm^{-3} and its production rate 2.8×10^6 cm^{-3} s^{-1} during these events (on average). Sulphuric acid proxy calculations based on sulphur dioxide concentrations and solar irradiance indicate that sulphuric acid cannot solely explain the growth of the particles. Potential contributors to growth are various organic vapours that are presumably abundant in

São Paulo and some of which are semi-volatile. We also observed evaporation from the sub-micron aerosol population as the modal diameter of the Aitken mode particles decreased. Semi-volatile vapours would explain the observation.

Based on these results we decided to continue our measurements in the city of São Paulo since more experimental evidence is needed to corroborate these observations.

Acknowledgements. "The effects of intensive BIO-Fuel production and USE on regional air quality and global climate" (BIOFUSE) was supported by the Academy of Finland via the Sustainable Energy Research Programme (SusEn, project number 1133603) and by the Brazilian National Council for Scientific and Technological Development (CNPq). Additional financial support by the Academy of Finland Centre of Excellence program (project no 1118615) and European Research Council (ERC) project ATMNUCLE are gratefully acknowledged. We also like to gratefully acknowledge Companhia de Tecnologia e Saneamento Ambiental do Estado de São Paulo (CETESB) for providing air pollution data, Laboratório de Micrometeorologia do IAG/USP, and Estação Meteorológica do IAG/USP for providing us with meteorological data. Tuukka Petäjä acknowledges funding from Academy of Finland, project 139656. Finally, Maria de Fatima Andrade is thankfully acknowledged for all her help with the data, her patience and her local knowledge.

References

Aalto, P., Hämeri, K., Becker, E., Weber, R., Salm, J., Mäkelä, J. M., Hoell, C., O'Dowd, C. D., Karlsson, H., Hansson, H. C., Väkevä, M., Koponen, I. K., Buzorius, G., and Kulmala, M.: Physical characterization of aerosol particles during nucleation events, Tellus B, 53, 344–358, 2001.

Agarwal, J. K. and Sem G. J.: Generating Submicron Monodispersc Aerosol for Instrument Calibration, TSI Quarterly, TSI Incorporated, St. Paul, MN 55164, USA, Volume IV, 2–8, 1978.

Allen, A. G., McGonigle, A. J. S., Cardoso, A. A., Machado, C. M. D., Davison, B., Paterlini, W. C., da Rocha, G. O., and de Andrade, J. B.: Influence of sources and meteorology on surface concentrations of gases and aerosols in a coastal industrial complex, J. Brazil Chem. Soc., 20, 214–221, 2009.

Anderson, T. L. and Ogren, J. A.: Determining aerosol radiative properties using the TSI 3563 integrating nephelometer, Aerosol. Sci. Tech., 29, 57–69, 1998.
Cabada, J. C., Khlystov, A., Wittig, A. E., Pilinis, C., and Pandis, S. N.: Light scattering by fine particles during the Pittsburgh Air Quality Study: measurements and modeling, J. Geophys. Res.-Atmos., 109, D16S03, doi:10.1029/2003JD004155, 2004.
CETESB: Relatório de Qualidade do Ar no Estado de São Paulo 2007: Série Relatórios, CETESB, São Paulo, SP, Brazil, ISSN 0103–4103, 2008.
Clarke, A. and Kapustin, V.: Hemispheric aerosol vertical profiles: anthropogenic impacts on optical depth and cloud nuclei, Science, 330, 1047–1047, 2010.
Coêlho, M. S. Z. S., Gonçalves, F. L. T., and Latorre, M. R. D. O.: Statistical analysis aiming at predicting respiratory tract disease hospital admissions from environmental variables in the city of São Paul, 2010, Journal of Environmental and Public Health, 209270, doi:10.1155/2010/209270, 2010.
Colon, M., Pleil, J. D., Hartlage, T. A., Guardani, M. L., and Martins, M. H.: Survey of volatile organic compounds associated with automative emissions in the urban airshed of Sao Paulo, Brazil, Atmos. Environ., 35, 4017–4031, 2001.
Dal Maso, M., Kulmala, M., Lehtinen, K. E. J., Mäkelä, J. M., Aalto, P., and O'Dowd, C. D.: Condensation and coagulation sinks and formation of nucleation mode particles in coastal and boreal forest boundary layers, J. Geophys. Res.-Atmos., 107, 8097, doi:10.1029/2001JD001053, 2002.
Dal Maso, M., Kulmala, M., Riipinen, I., Wagner, R., Hussein, T., Aalto, P. P., and Lehtinen, K. E. J.: Formation and growth of fresh atmospheric aerosols: eight years of aerosol size distribution data from SMEAR II, Hyytiala, Finland, Boreal Environ. Res., 10, 323–336, 2005.
Davidson, C., Phalen, R., and Solomon, P.: Airborne particulate matter and human health: a review, Aerosol. Sci. Tech., 39, 737–749, doi:10.1080/02786820500191348, 2005.
Dunn, M. J., Jimenez, J. L., Baumgardner, D., Castro, T., McMurry, P. H., and Smith, J. N.: Measurements of Mexico City nanoparticle size distributions: observations of new particle formation and growth, Geophys. Res. Lett., 31, L10102, doi:10.1029/2004GL019483, 2004.
Eck, T. F., Holben, B. N., Reid, J. S., Dubovik, O., Smirnov, A., O'Neill, N. T., Slutsker, I., and Kinne, S.: Wavelength dependence of the optical depth of biomass burning, urban, and desert dust aerosols, J. Geophys. Res.-Atmos., 104, 31333–31349, 1999.
Farrell, A. E.: Ethanol can contribute to energy and environmental goals (vol 311, pg 506,

2006), Science, 312, 1748–1748, 2006.
Fuchs, N. A.: On the stationary charge distribution on aerosol particles in a bipolar ionic atmosphere, Pure Appl. Geophys., 56, 185–193, 1963.
Garland, R. M., Schmid, O., Nowak, A., Achtert, P., Wiedensohler, A., Gunthe, S. S., Takegawa, N., Kita, K., Kondo, Y., Hu, M., Shao, M., Zeng, L. M., Zhu, T., Andreae, M. O., and Poeschl, U.: Aerosol optical properties observed during Campaign of Air Quality Research in Beijing 2006 (CAREBeijing-2006): characteristic differences between the inflow and outflow of Beijing city air, J. Geophys. Res.-Atmos., 114, D00G04, doi:10.1029/2008JD010780, 2009.
Graham, L. A., Belisle, S. L., and Baas, C.: Emissions from light duty gasoline vehicles operating on low blend ethanol gasoline and E85, Atmos. Environ., 42, 4498–4516, doi:10.1016/j.atmosenv.2008.01.061, 2008.
Gurjar, B. R., Butler, T. M., Lawrence, M. G., and Lelieveld, J.: Evaluation of emissions and air quality in megacities, Atmos. Environ., 42, 1593–1606, doi:10.1016/j.atmosenv.2007.10.048, 2008.
Haagensmit, A. J.: Chemistry and physiology of Los-Angeles smog, Ind. Eng. Chem., 44, 1342–1346, 1952.
Hansen, J., Sato, M., and Ruedy, R.: Radiative forcing and climate response, J. Geophys. Res.-Atmos., 102, 6831–6864, 1997.
Haywood, J. and Boucher, O.: Estimates of the direct and indirect radiative forcing due to tropospheric aerosols: a review, Rev. Geophys., 38, 513–543, 2000.
Herrmann, P. and Hänel, G.: Wintertime optical properties of atmospheric particles and weather, Atmos. Environ., 31, 4053–4062, 1997.
Hirsikko, A., Laakso, L., Horrak, U., Aalto, P. P., Kerminen, V. M., and Kulmala, M.: Annual and size dependent variation of growth rates and ion concentrations in boreal forest, Boreal Environ. Res., 10, 357–369, 2005.
Hoppel, W. A.: Determination of the aerosol size distribution from the mobility distribution of the charged fraction of aerosols, J. Aerosol Sci., 9, 41–54, doi:10.1016/0021-8502(78)90062-9, 1978.
Hussein, T., Dal Maso, M., Petäjä, T., Koponen, I. K., Paatero, P., Aalto, P. P., Hämeri, K., and Kulmala, M.: Evaluation of an automatic algorithm for fitting the particle number size distributions, Boreal Environ. Res., 10, 337–355, 2005.
Hyvärinen, A.-P., Lihavainen, H., Komppula, M., Sharma, V. P., Kerminen, V. M., Pan-

war, T. S., and Viisanen, Y.: Continuous measurements of optical properties of atmospheric aerosols in Mukteshwar, Northern India, J. Geophys. Res.-Atmos., 114, D08207, doi:10.1029/2008JD011489, 2009.
Hyvärinen, A.-P., Lihavainen, H., Komppula, M., Panwar, T. S., Sharma, V. P., Hooda, R. K., and Viisanen, Y.: Aerosol measurements at the Gual Pahari EUCAARI station: preliminary results from in-situ measurements, Atmos. Chem. Phys., 10, 7241–7252, doi:10.5194/acp-10-7241-2010, 2010.
IPCC: Climate Change 2007: The Physical Science Basis, Contribution of Working Group I to the Fourth Assessment Report of the Intergovernmental Panel on Climate Change, Cambridge University Press, Cambridge, United Kingdom and New York, NY, USA, 2007.
Jacobson, M. Z.: Strong radiative heating due to the mixing state of black carbon in atmospheric aerosols, Nature, 409, 695–697, 2001.
Jacobson, M. Z.: Effects of ethanol (E85) versus gasoline vehicles on cancer and mortality in the United States, Environ. Sci. Technol., 41, 4150–4157, doi:10.1021/es062085v, 2007.
Jimenez, J. L., Canagaratna, M. R., Donahue, N. M., Prevot, A. S. H., Zhang, Q., Kroll, J. H., DeCarlo, P. F., Allan, J. D., Coe, H., Ng, N. L., Aiken, A. C., Docherty, K. S., Ulbrich, I. M., Grieshop, A. P., Robinson, A. L., Duplissy, J., Smith, J. D., Wilson, K. R., Lanz, V. A., Hueglin, C., Sun, Y. L., Tian, J., Laaksonen, A., Raatikainen, T., Rautiainen, J., Vaattovaara, P., Ehn, M., Kulmala, M., Tomlinson, J. M., Collins, D. R., Cubison, M. J., Dunlea, E. J., Huffman, J. A., Onasch, T. B., Alfarra, M. R., Williams, P. I., Bower, K., Kondo, Y., Schneider, J., Drewnick, F., Borrmann, S., Weimer, S., Demerjian, K., Salcedo, D., Cottrell, L., Griffin, R., Takami, A., Miyoshi, T., Hatakeyama, S., Shimono, A., Sun, J. Y., Zhang, Y. M., Dzepina, K., Kimmel, J. R., Sueper, D., Jayne, J. T., Herndon, S. C., Trimborn, A. M., Williams, L. R., Wood, E. C., Middlebrook, A. M., Kolb, C. E., Baltensperger, U., and Worsnop, D. R.: Evolution of organic aerosols in the atmosphere, Science, 326, 1525–1529, doi:10.1126/science.1180353, 2009.
Kalafut-Pettibone, A. J., Wang, J., Eichinger, W. E., Clarke, A., Vay, S. A., Blake, D. R., and Stanier, C. O.: Size-resolved aerosol emission factors and new particle formation/growth activity occurring in Mexico City during the MILAGRO 2006 Campaign, Atmos. Chem. Phys., 11, 8861–8881, doi:10.5194/acp-11-8861-2011, 2011.
Kerminen, V. M., Pirjola, L., and Kulmala, M.: How significantly does coagulational scavenging limit atmospheric particle production?, J. Geophys. Res.-Atmos., 106, 24119–24125, 2001.
Kulmala, M.: How particles nucleate and grow, Science, 302, 1000–1001, 2003.

Kulmala, M. and Tammet, H.: Finnish-Estonian air ion and aerosol workshops, Boreal Environ. Res., 12, 237–245, 2007.
Kulmala, M., Dal Maso, M., Mäkelä, J. M., Pirjola, L., Väkevä, M., Aalto, P., Miikkulainen, P., Hämeri, K., and O'Dowd, C. D.: On the formation, growth and composition of nucleation mode particles, Tellus B, 53, 479–490, 2001.
Kulmala, M., Vehkamaki, H., Petäjä, T., Dal Maso, M., Lauri, A., Kerminen, V. M., Birmili, W., and McMurry, P. H.: Formation and growth rates of ultrafine atmospheric particles: a review of observations, J. Aerosol Sci., 35, 143–176, doi:10.1016/j.jaerosci.2003.10.003, 2004.
Kulmala, M., Petäjä, T., Mönkkönen, P., Koponen, I. K., Dal Maso, M., Aalto, P. P., Lehtinen, K. E. J., and Kerminen, V.-M.: On the growth of nucleation mode particles: source rates of condensable vapor in polluted and clean environments, Atmos. Chem. Phys., 5, 409–416, doi:10.5194/acp-5-409-2005, 2005.
Laakso, L., Koponen, I. K., Mönkkönen, P., Kulmala, M., Kerminen, V., Wehner, B., Wiedensohler, A., Wu, Z., and Hu, M.: Aerosol particles in the developing world; a comparison between New Delhi in India and Beijing in China, Water Air Soil Poll., 173, 5–20, doi:10.1007/s11270-005-9018-5, 2006.
Lohmann, U. and Feichter, J.: Global indirect aerosol effects: a review, Atmos. Chem. Phys., 5, 715–737, doi:10.5194/acp-5-715-2005, 2005.
Manninen, H. E., Nieminen, T., Riipinen, I., Yli-Juuti, T., Gagné, S., Asmi, E., Aalto, P. P., Petäjä, T., Kerminen, V.-M., and Kulmala, M.: Charged and total particle formation and growth rates during EUCAARI 2007 campaign in Hyytiälä, Atmos. Chem. Phys., 9, 4077–4089, doi:10.5194/acp-9-4077-2009, 2009a.
Manninen, H. E., Petäjä, T., Asmi, E., Riipinen, I., Nieminen, T., Mikkilä, J., Horrak, U., Mirme, A., Mirme, S., Laakso, L., Kerminen, V., and Kulmala, M.: Long-term field measurements of charged and neutral clusters using Neutral cluster and Air Ion Spectrometer (NAIS), Boreal Environ. Res., 14, 591–605, 2009b.
Mészáros, E., Molnar, A., and Ogren, J.: Scattering and absorption coefficients vs. chemical composition of fine atmospheric aerosol particles under regional conditions in Hungary, J. Aerosol Sci., 29, 1171–1178, 1998.
Mirme, A., Tamm, E., Mordas, G., Vana, M., Uin, J., Mirme, S., Bernotas, T., Laakso, L., Hirsikko, A., and Kulmala, M.: A wide-range multi-channel air ion spectrometer, Boreal Environ. Res., 12, 247–264, 2007.
Mönkkönen, P., Koponen, I. K., Lehtinen, K. E. J., Hämeri, K., Uma, R., and Kulmala, M.:

Measurements in a highly polluted Asian mega city: observations of aerosol number size distribution, modal parameters and nucleation events, Atmos. Chem. Phys., 5, 57–66, doi:10.5194/acp-5-57-2005, 2005.

Müller, T., Henzing, J. S., de Leeuw, G., Wiedensohler, A., Alastuey, A., Angelov, H., Bizjak, M., Collaud Coen, M., Engström, J. E., Gruening, C., Hillamo, R., Hoffer, A., Imre, K., Ivanow, P., Jennings, G., Sun, J. Y., Kalivitis, N., Karlsson, H., Komppula, M., Laj, P., Li, S.-M., Lunder, C., Marinoni, A., Martins dos Santos, S., Moerman, M., Nowak, A., Ogren, J. A., Petzold, A., Pichon, J. M., Rodriquez, S., Sharma, S., Sheridan, P. J., Teinilä, K., Tuch, T., Viana, M., Virkkula, A., Weingartner, E., Wilhelm, R., and Wang, Y. Q.: Characterization and intercomparison of aerosol absorption photometers: result of two intercomparison workshops, Atmos. Meas. Tech., 4, 245–268, doi:10.5194/amt-4-245-2011, 2011.

Neitola, K., Asmi, E., Komppula, M., Hyvärinen, A.-P., Raatikainen, T., Panwar, T. S., Sharma, V. P., and Lihavainen, H.: New particle formation infrequently observed in Himalayan foothills – why?, Atmos. Chem. Phys., 11, 8447–8458, doi:10.5194/acp-11-8447-2011, 2011.

Nel, A.: Air pollution-related illness: effects of particles, Science, 308, 804–806, doi:10.1126/science.1108752, 2005.

Nieminen, T., Manninen, H. E., Sihto, S.-L., Yli-Juuti, T., Mauldin, III, R. L., Petäjä, T., Riipinen, I., Kerminen, V. M., and Kulmala, M.: Connection of sulfuric acid to atmospheric nucleation in boreal forest, Environ. Sci. Technol., 43, 4715–4721, doi:10.1021/es803152j, 2009.

Nieminen, T., Lehtinen, K. E. J., and Kulmala, M.: Sub-10 nm particle growth by vapor condensation – effects of vapor molecule size and particle thermal speed, Atmos. Chem. Phys., 10, 9773–9779, doi:10.5194/acp-10-9773-2010, 2010.

de Oliveira, A. P., Machado, A. J., Escobedo, J. F., and Soares, J.: Diurnal evolution of solar radiation at the surface in the city of Sao Paulo: seasonal variation and modeling, Theor. Appl. Climatol., 71, 231–250, 2002.

Orlando, J. P., Alvim, D. S., Yamazaki, A., Correa, S. M., and Gatti, L. V.: Ozone precursors for the Sao Paulo Metropolitan Area, Sci. Total Environ., 408, 1612–1620, doi:10.1016/j.scitotenv.2009.11.060, 2010.

Paredes-Miranda, G., Arnott, W. P., Jimenez, J. L., Aiken, A. C., Gaffney, J. S., and Marley, N. A.: Primary and secondary contributions to aerosol light scattering and absorption in Mexico City during the MILAGRO 2006 campaign, Atmos. Chem. Phys., 9, 3721–3730, doi:10.5194/acp-9-3721-2009, 2009.

Petäjä, T., Mauldin, III, R. L., Kosciuch, E., McGrath, J., Nieminen, T., Paasonen, P., Boy, M., Adamov, A., Kotiaho, T., and Kulmala, M.: Sulfuric acid and OH concentrations in a boreal forest site, Atmos. Chem. Phys., 9, 7435–7448, doi:10.5194/acp-9-7435-2009, 2009.

Petzold, A., Schloesser, H., Sheridan, P. J., Arnott, W. P., Ogren, J. A., and Virkkula, A.: Evaluation of multiangle absorption photometry for measuring aerosol light absorption, Aerosol. Sci. Tech., 39, 40–51, doi:10.1080/027868290901945, 2005.

Poeschl, U., Martin, S. T., Sinha, B., Chen, Q., Gunthe, S. S., Huffman, J. A., Borrmann, S., Farmer, D. K., Garland, R. M., Helas, G., Jimenez, J. L., King, S. M., Manzi, A., Mikhailov, E., Pauliquevis, T., Petters, M. D., Prenni, A. J., Roldin, P., Rose, D., Schneider, J., Su, H., Zorn, S. R., Artaxo, P., and Andreae, M. O.: Rainforest aerosols as biogenic nuclei of clouds and precipitation in the Amazon, Science, 329, 1513–1516, doi:10.1126/science.1191056, 2010.

Ramanathan, V. and Carmichael, G.: Global and regional climate changes due to black carbon, Nat. Geosci., 1, 221–227, doi:10.1038/ngeo156, 2008.

Ramanathan, V., Crutzen, P. J., Kiehl, J. T., and Rosenfeld, D.: Atmosphere – aerosols, climate, and the hydrological cycle, Science, 294, 2119–2124, 2001.

Salcedo, D., Onasch, T. B., Dzepina, K., Canagaratna, M. R., Zhang, Q., Huffman, J. A., DeCarlo, P. F., Jayne, J. T., Mortimer, P., Worsnop, D. R., Kolb, C. E., Johnson, K. S., Zuberi, B., Marr, L. C., Volkamer, R., Molina, L. T., Molina, M. J., Cardenas, B., Bernabé, R. M., Márquez, C., Gaffney, J. S., Marley, N. A., Laskin, A., Shutthanandan, V., Xie, Y., Brune, W., Lesher, R., Shirley, T., and Jimenez, J. L.: Characterization of ambient aerosols in Mexico City during the MCMA-2003 campaign with Aerosol Mass Spectrometry: results from the CENICA Supersite, Atmos. Chem. Phys., 6, 925–946, doi:10.5194/acp-6-925-2006, 2006.

Seinfeld, J. H. and Pandis, S. N.: Atmospheric Chemistry and Physics From Air Pollution to Climate Change, 2nd edition., John Wiley & Sons, New York, 2006.

Sem, G.: Design and performance characteristics of three continuous-flow condensation particle counters: a summary, Atmos. Res., 62, 267–294, doi:10.1016/S0169-8095(02)00014-5, 2002.

Silva Júnior, R. S., de Oliveira, M. G. L., and Andrade, M. D. F.: Weekend/weekday differences 30 in concentrations of ozone, nox, and non-methane hydrocarbon in the metropolitan area of So Paulo, Revista Brasileira de Meteorologia, 24, 100-110, 2009.

Sipilä, M., Berndt, T., Petäjä, T., Brus, D., Vanhanen, J., Stratmann, F., Patokoski, J., Mauldin, III, R. L., Hyvärinen, A., Lihavainen, H., and Kulmala, M.: The role of sulfuric acid in atmospheric

nucleation, Science, 327, 1243–1246, doi:10.1126/science.1180315, 2010.
Tammet, H. and Kulmala, M.: Simulation tool for atmospheric aerosol nucleation bursts, J. Aerosol Sci., 36, 173–196, doi:10.1016/j.jaerosci.2004.08.004, 2005.
Virkkula, A., Hirsikko, A., Vana, M., Aalto, P. P., Hillamo, R., and Kulmala, M.: Charged particle size distributions and analysis of particle formation events at the Finnish Antarctic research station Aboa, Boreal Environ. Res., 12, 397–408, 2007.
Weber, R., Marti, J., McMurry, P., Eisele, F., Tanner, D., and Jefferson, A.: Measured atmospheric new particle formation rates: implications for nucleation mechanisms RID A-8245-2008, Chem. Eng. Commun., 151, 53–64, doi:10.1080/00986449608936541, 1996.
Wehner, B., Wiedensohler, A., Tuch, T. M., Wu, Z. J., Hu, M., Slanina, J., and Kiang, C. S.: Variability of the aerosol number size distribution in Beijing, China: new particle formation, dust storms, and high continental background, Geophys. Res. Lett., 31, L22108, doi:10.1029/2004GL021596, 2004.
Wehner, B., Petäjä, T., Boy, M., Engler, C., Birmili, W., Tuch, T., Wiedensohler, A., and Kulmala, M.: The contribution of sulfuric acid and non-volatile compounds on the growth of freshly formed atmospheric aerosols, Geophys. Res. Lett., 32, L17810, doi:10.1029/2005GL023827, 2005.
Winklmayr, W., Reischl, G. P., Lindner, A. O., and Berner, A.: A new electromobility spectrometer for the measurement of aerosol size distributions in the size range from 1 to 1000 Nm, J. Aerosol Sci., 22, 289–296, 1991.
Zhang, S. H. and Flagan, R. C.: Resolution of the radial differential mobility analyzer for ultrafine particles, J. Aerosol Sci., 27, 1179–1200, 1996.

Table 1. A summary table of observed new particle formation events observed. They were classified according to Dal Maso et al. (2005). The growth rates (GR) and particle fluxes (J) with two values are calculated from ion spectrometer data for both polarities (+ and −). $J_{2,TOT}$ is calculated from artificially charged (negative) particles. The condensation sink (CS), vapour abundance (C_{vap}) and production rate (Q) are calculated from DMPS data. For further explanations, see the methods section. The days mentioned in the table are all in year 2010.

Date	Type	GR_{1-3} (+/−)	GR_{3-7} (+/−)	GR_{7-20} (+/−)	GR_{6-20}	J_2 (+/−)	$J_{2,TOT}$	J_6	CS	C_{vap}	H_2SO_4 proxy	Q
		(nm h^{-1})				(cm^{-3} s^{-1})			(10^{-3} s^{-1})	(10^8 cm^{-3})	(10^7 cm^{-3})	(10^6 cm^{-3} s^{-1})
10 Oct	Ia	7.0/8.0	14.1/8.3	48.5/33.8	25.1	0.13/0.08	10.3	11.2	5.7	4.3	1.4	2.5
12 Oct	II	–	–	–	–	–	–	–	–	–	–	–
31 Oct	Ib	–	–	–	–	–	–	–	–	–	–	–
2 Nov	Ia	6.1/4.7	5.3/–	7.0/7.2	9.3	0.25/0.04	55.7	11.4	16.7	1.6	0.9	2.7
3 Nov	Ib	–	–	–	–	–	–	–	–	–	–	–
7 Nov	Ia	6.3/4.1	10.3/5.8	12.5/10.8	16.1	0.25/0.12	23.1	18.5	15.7	2.8	1.1	4.4
15 Nov	Ia	5.0/3.9	16.9/7.1	14.1/5.7	10.7	0.14/0.08	10.3	4.5	9.9	1.8	1.1	1.8
12 Dec	Undef.	–	–	–	–	–	–	–	–	–	–	–
31 Dec	II	–	–	–	–	–	–	–	–	–	–	–
1 Jan	Ib	–	–	–	–	–	–	–	–	–	–	–
Mean:		6.2/4.4	12.2/7.1	13.3/9.0	15.3	0.19/0.08	24.9	11.4	12.0	2.6	1.1	2.8

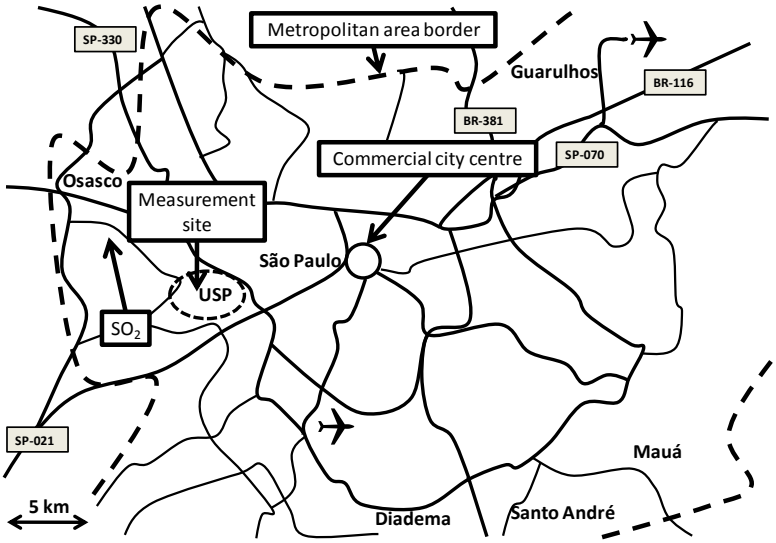

Fig. 1. Map of the metropolitan area of São Paulo. The measurement site is west of the geographical city centre. The Osasco sulphur dioxide (SO_2) monitoring station is north west of the measurement site. The metropolitan area of São Paulo is inhabited by 20 million people.

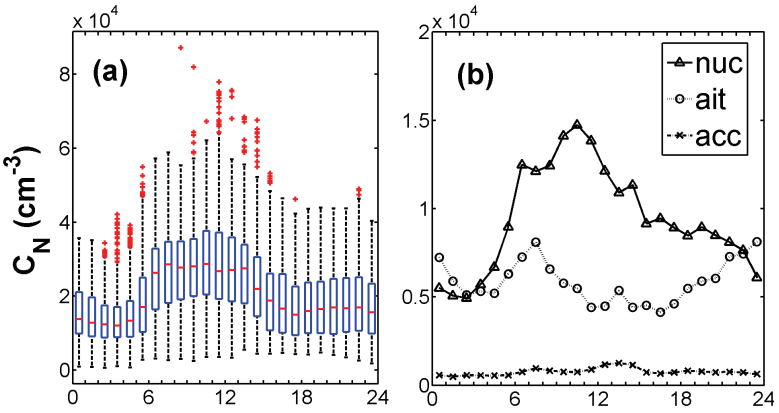

Fig. 2. Three month diurnal behaviour of the **(a)** total particle number concentration and **(b)** the nucleation (nuc), Aitken (aik), and accumulation (acc) mode particle number concentrations using 5 min average data. The modal number concentrations were obtained by fitting three modes to the number size distributions. The upper and lower box edges in the **(a)** part of the figure are the the 75th and 25th percentiles with a red line in between, showing the median value. The black whiskers indicate the statistical edges of the data.

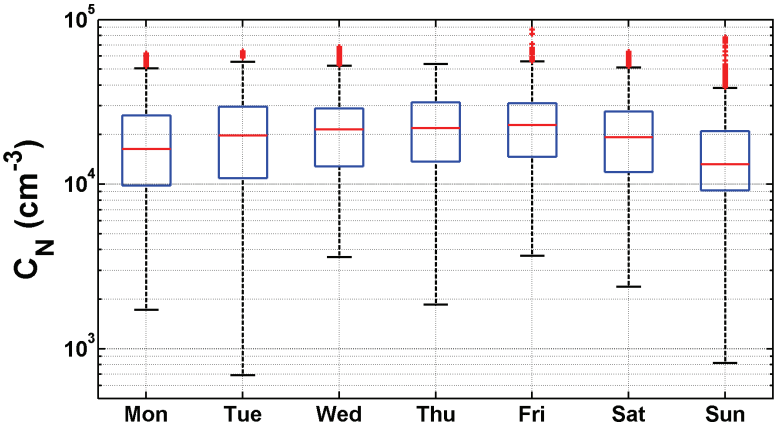

Fig. 3. The weekly cycle of the total particle number concentration. Sundays had the lowest and Fridays the highest concentrations, 1.3×10^4 and 2.3×10^4 cm^{-3}, respectively.

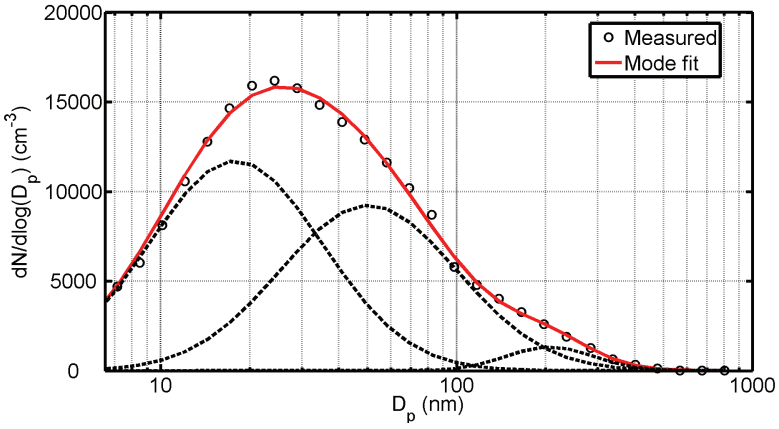

Fig. 4. Three month median number size distribution with three modes fitted to the data. The modal peaks of the nucleation, Aitken, and accumulation mode particles are at 18, 50 and 206 nm, respectively. The median modal particle concentrations are 8600, 6900 and 500 cm^{-3}. The width (σ) of the mode fits are 1.96, 1.99 and 1.40.

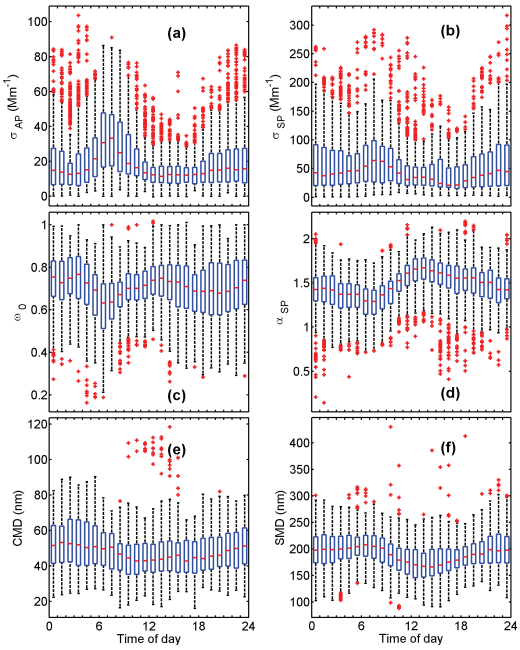

Fig. 5. Diurnal cycle of **(a)** light absorption coefficients, **(b)** light scattering coefficients, and **(c)** single-scattering albedo at 637 nm. Ångström exponents **(d)** were calculated from 450 and 700 nm light scattering coefficients. **(e)** Count mean diameters (CMD) and **(f)** Surface mean diameters (SMD) were also plotted.

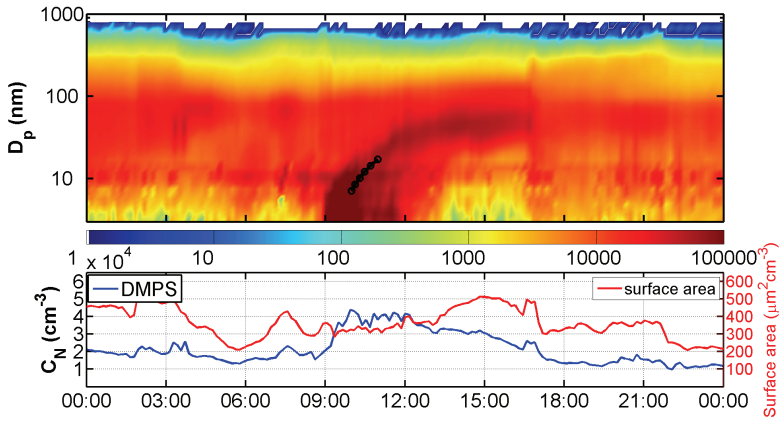

Fig. 6. The nucleation event measured on 2 November 2010. A growth rate (GR_{6-20}) of 9.3 nm h^{-1} was calculated using DMPS data from 6 to 20 nm indicated by black circles. The split between NAIS and DMPS data in the picture is at 15 nm.

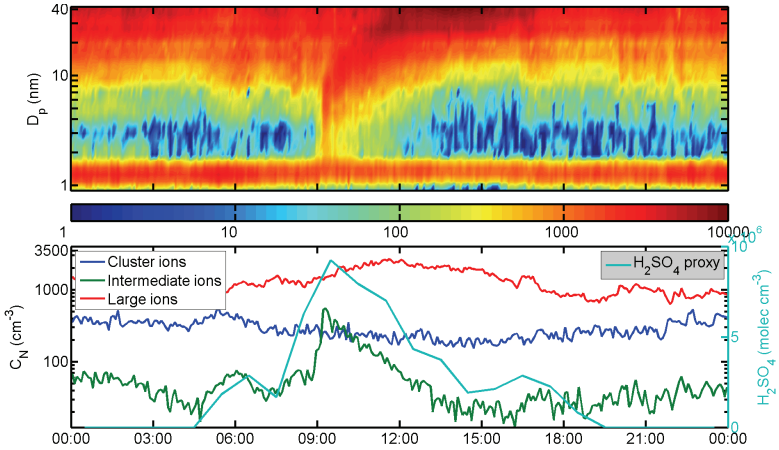

Fig. 7. The upper panel shows naturally positively charged particle number size distribution (0.8–42 nm) measured with the NAIS on 2 November 2010. The lower panel shows number concentrations of cluster (< 1.8 nm), intermediate (1.8–7 nm) and large (7–42 nm) ions. On the right axis the sulphuric acid (H_2SO_4) proxy concentration is shown.

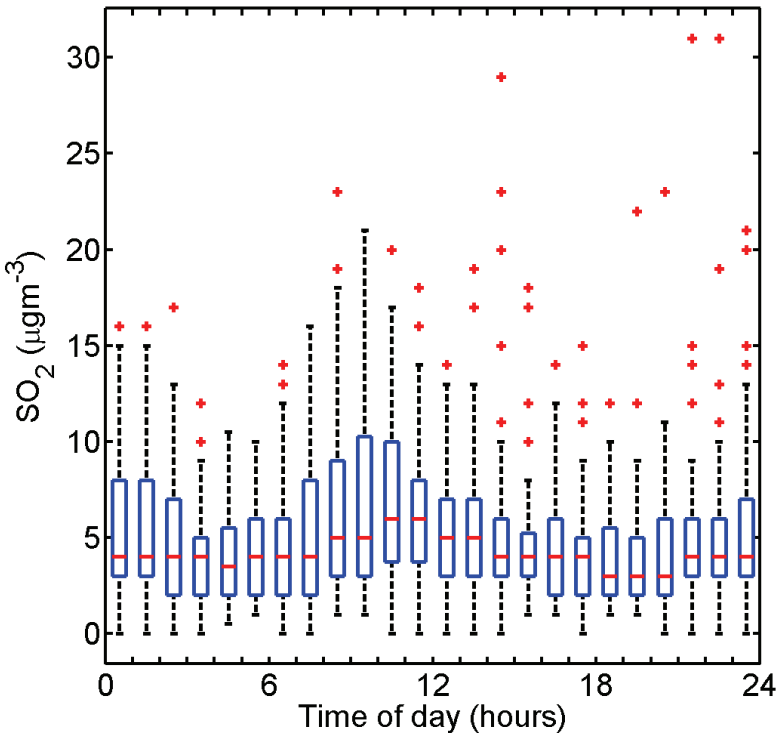

Fig. 8. The diurnal behaviour of sulphur dioxide (SO_2) measured at the Osasco monitoring station used for the sulphuric acid (H_2SO_4) proxy.

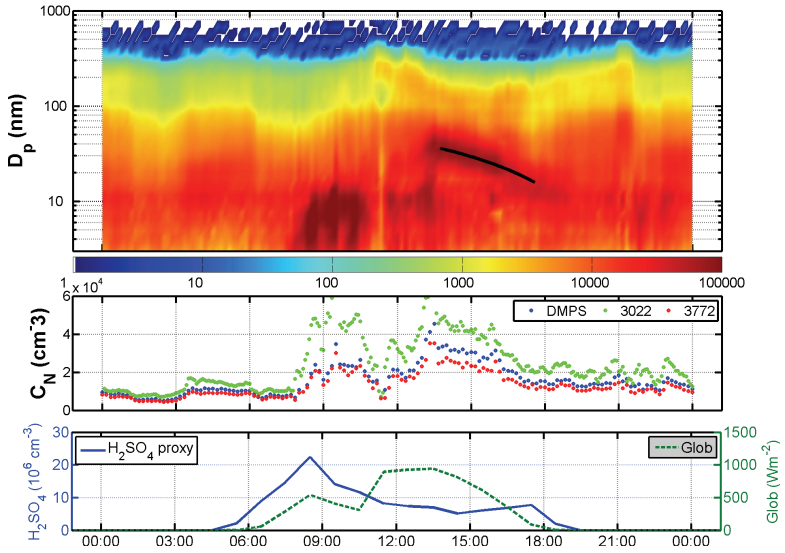

Fig. 9. Class II type event during morning hours and a shrinking mode in the early afternoon on 12 October 2010. During the evaporation (from 14:00 to 17:00 LT) the total particle concentration declines constantly. The evaporation rate of the shrinking mode was calculated to be 5.2 nm h^{-1}. The split between NAIS and DMPS data in the picture is at 15 nm.